Methods

Environmental Data

Atmospheric and sea-state parameters were acquired from the European Center for Medium-Range Weather Forecast (ECMWF) ERA5 reanalysis, providing data on a regular latitude-longitude grid at 0.25° x 0.25° spatial resolution and hourly temporal resolution (Hersbach, H. et al., 2018a; Hersbach, H. et al., 2018b). The area of interest for this study is the latitude/longitude box with coordinates 3.25°-7°E and 51°-54.25°N, which includes the entire North Sea coast of The Netherlands, and the temporal interval is June-July 2019-2020, corresponding to observations of soaring behavior in GPS and radar retrievals. The parameters extracted from ERA5 data were instantaneous surface sensible heat flux (ISHF*) [Wm^{-2}], air temperature at 2 m above surface (T_a) [°K], sea surface temperature (SST) [°K], wind speed u- and v- components at 10 m above the surface (u_{10m} and v_{10m}, respectively) [ms^{-1}], mean sea level pressure [hPa], total cloud cover [0-1], total precipitation [m]. Note that the ECMWF convection for vertical fluxes is positive downwards. Since we are interested in soaring over the North Sea, we define the flux ISHF as the negative of ISHF*, which represents a positive transfer of heat from the sea surface to the atmosphere. Hence, the magnitude of ISHF depends mainly on the difference between SST and T_a, but also on the wind speed U near the surface. Faizal and Ahmed (2011) provided a similar approximation for the sea surface sensible heat flux Q_h that considers the mentioned parameters: $Q_h = 1.88\ U\ (SST - T_a)$, valid for the Pacific Ocean. Further approximations were proposed in literature to approximate the dependency of the sensible heat flux on the wind speed as either a constant, linear or quadratic relationship (Kalinowska, 2019). In this study we will refer mainly to Q_h.
Wind components were selected in proximity of the sea surface to match both the properties of the radar observations and known flight heights of the relevant bird species: we expected flight altitudes of most species to be close to the sea surface during local movements (Johnston et al. 2014; Corman and Garthe 2014; Ross-Smith et al. 2016; Borkenhagen et al. 2017). The wind speed u-component is the zonal wind (wind from the west is positive) and the v-component is the meridional wind (wind from south is positive). To calculate Q_h the wind speed at 2 m above the surface was calculated using a power low to relate wind speed components at 2 m and at 10 m (Hsu et al., 1993).

Discussion

Atmospheric Conditions

Soaring has been observed in both radar and GPS retrievals on some specific days during the summer of 2019 and 2020. Luchterduinen windfarm radar data and GPS observations around IJmuiden agree on more-than-average soaring activity on, for example, 15-07-2020. Similarly, Gemini windfarm radar data and GPS observations around Schiermonnikoog agree on soaring activity in the days 20,21,22-07-2020. For these dates, surface pressure charts showing pressure and weather fronts for Europe at 6-hour temporal resolution have been downloaded from the KNMI data center (https://www.knmi.nl/nederland-nu/klimatologie/daggegevens/weerkaarten), and time series of ERA5 atmospheric and sea-state parameters have been plotted for the two locations.

On 14-07-2020 at 06 UTC and at 12 UTC (Figures 1 and 2) a series of fronts are passing over the Netherlands: a warm front followed by a cold front and a occluded front, which is formed when the cold front (which travels faster) catches up with the warm front. These fronts are associated with atmospheric instability and mixing of different air masses (maritime and continental, https://www.metoffice.gov.uk/weather/learn-about/weather/atmosphere/air-masses/types). Schiermoonikoog time series for total cloud cover and total precipitation confirm that a precipitating system is traveling across the Netherlands during the day, leaving some precipitation at the ground (Figures 21 and 22). By the end of the day the fronts leave space to a trough coming from the North Sea and sweeping the coast of the Netherlands (Figures 3 and 4). Such trough, which brings cold maritime wet air from NW, lingers till the end of July 15th (Figures 5 to 8). The presence of such cold air in the upper atmosphere creates suitable conditions for the development of

thermals near the Dutch coast: the sea surface becomes warmer than the air above it from the end of July 14th (Figure 23), resulting in a positive difference of temperature (Figure 24), which drives an exchange of heat from the sea to the atmosphere (Markowski & Richardson, 2010).
A similar situation takes place between July 20st and 22nd near IJmuiden. A cold front from NW swipes the Netherlands on July 20th (Figures 9 to 11) leaving behind a trough at the end of the day and in the following days (Figures 12 to 20). During these days the sky above IJmuiden is quite clear and no precipitation is observed (Figures 25 and 26). Furthermore, the atmosphere gets colder than the SST (Figure 27 and 28), creating the same suitable conditions discussed above for the development of thermals.
Note that, in both cases described above, the wind intensity $U = \mathrm{sqrt}(u_{10m}^2 + v_{10m}^2)$ is not particularly high compared to monthly time series (Figures 29 and 32), but the wind is predominantly North-Westerly (Figures 31 and 32).

Bibliography

Faizal, Mohammed, and M. Rafiuddin Ahmed. “On the Ocean Heat Budget and Ocean Thermal Energy Conversion.” International Journal of Energy Research 35, no. 13 (2011): 1119–44. https://doi.org/10.1002/er.1885.

Hersbach, H., Bell, B., Berrisford, P., Biavati, G., Horányi, A., Muñoz Sabater, J., Nicolas, J., Peubey, C., Radu, R., Rozum, I., Schepers, D., Simmons, A., Soci, C., Dee, D., Thépaut, J-N. (2018a): ERA5 hourly data on single levels from 1979 to present. Copernicus Climate Change Service (C3S) Climate Data Store (CDS). (Accessed on 28-SEP-2021), 10.24381/cds.adbb2d47

Hersbach, H., Bell, B., Berrisford, P., Biavati, G., Horányi, A., Muñoz Sabater, J., Nicolas, J., Peubey, C., Radu, R., Rozum, I., Schepers, D., Simmons, A., Soci, C., Dee, D., Thépaut, J-N. (2018b): ERA5 hourly data on pressure levels from 1979 to present. Copernicus Climate Change Service (C3S) Climate Data Store (CDS). (Accessed on 28-SEP-2021), 10.24381/cds.bd0915c6

Hsu, S. A., Eric A. Meindl, and David B. Gilhousen. “Determining the Power-Law Wind-Profile Exponent under Near-Neutral Stability Conditions at Sea.” Journal of Applied Meteorology and Climatology 33, no. 6 (June 1, 1994): 757–65.

Kalinowska, Monika Barbara. “Effect of Water–Air Heat Transfer on the Spread of Thermal Pollution in Rivers.” Acta Geophysica 67, no. 2 (April 1, 2019): 597–619. https://doi.org/10.1007/s11600-019-00252-y.

Markowski, P., & Richardson, Y. (2010). *Mesoscale meteorology in midlatitudes*. Chichester: Wiley-Blackwell.

Figures

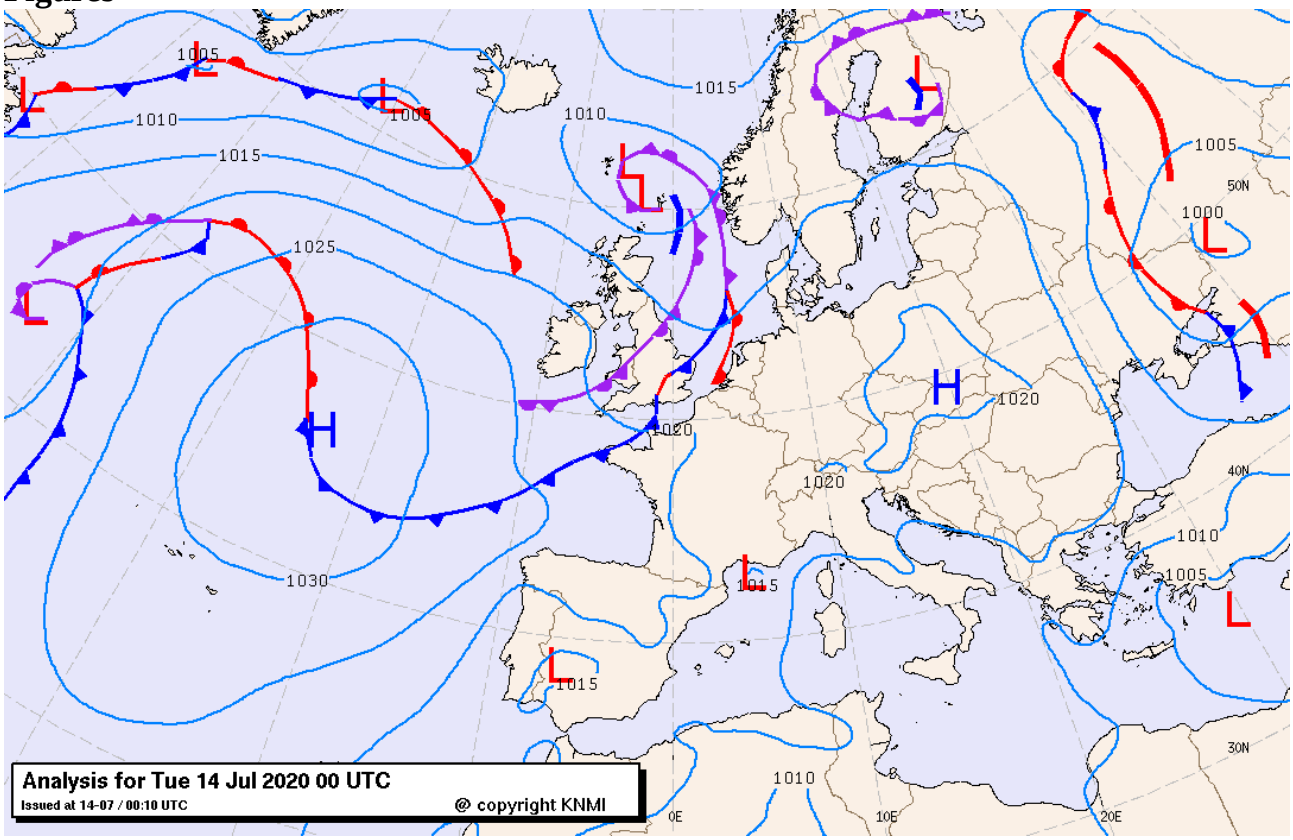

Figure 1. Surface pressure chart from KNMI data center. 14 July 2020 at 00 UTC.

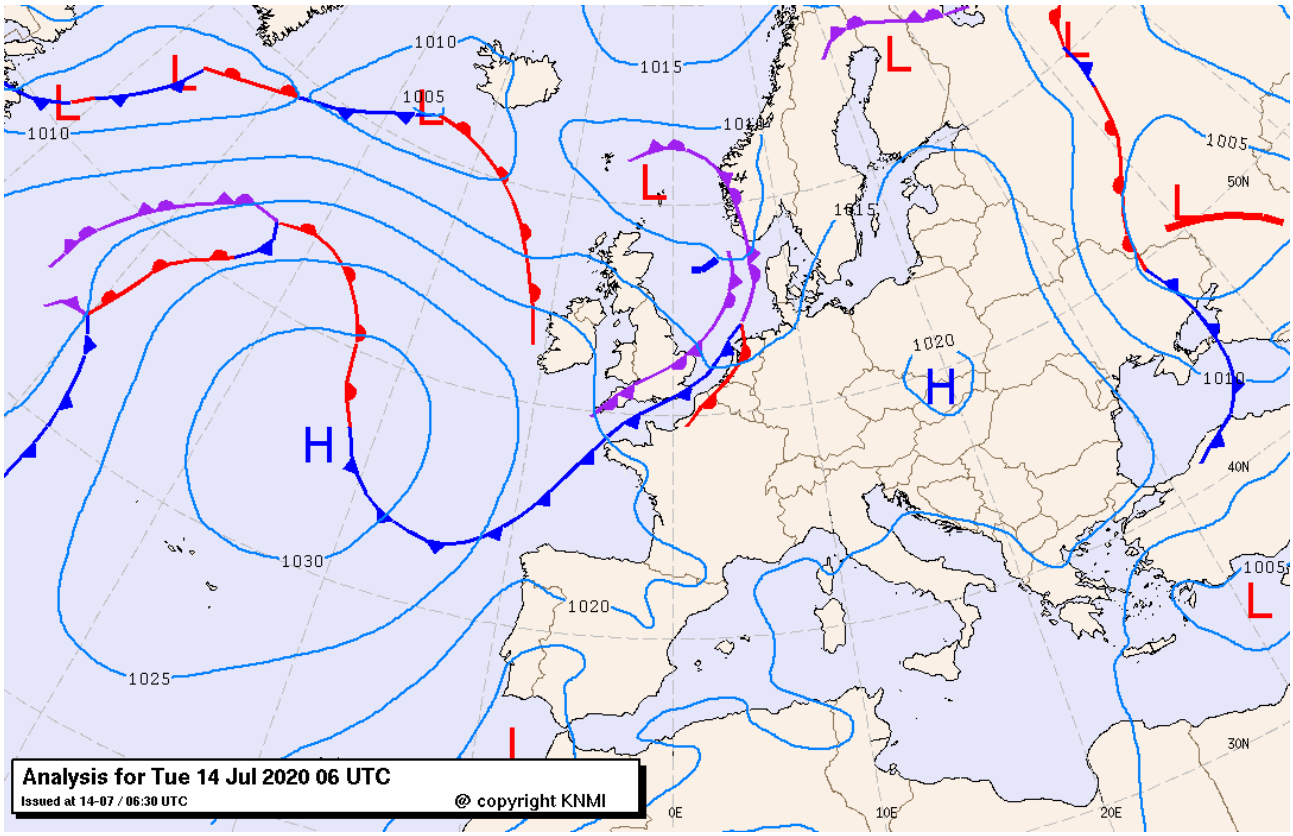

Figure 2. Surface pressure chart from KNMI data center. 14 July 2020 at 06 UTC.

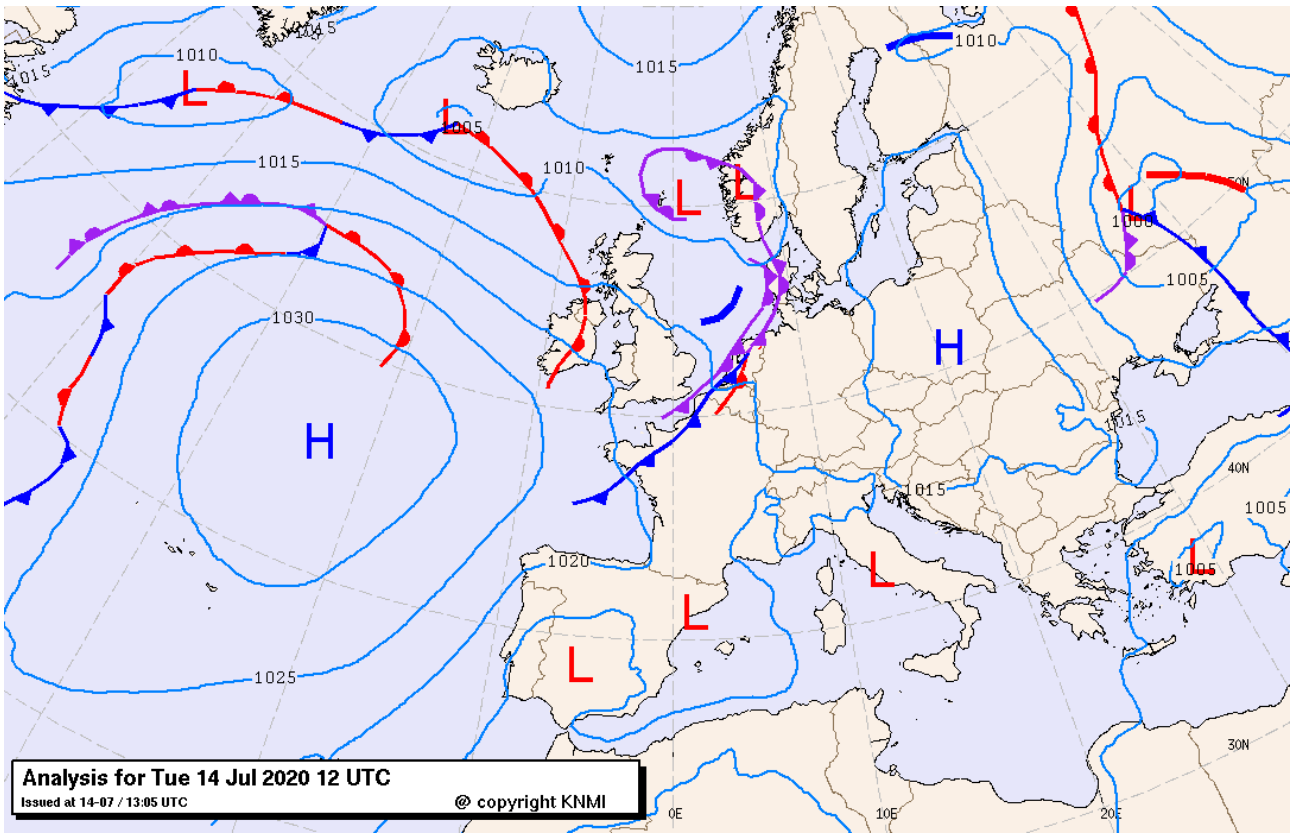

Figure 3. Surface pressure chart from KNMI data center. 14 July 2020 at 12 UTC.

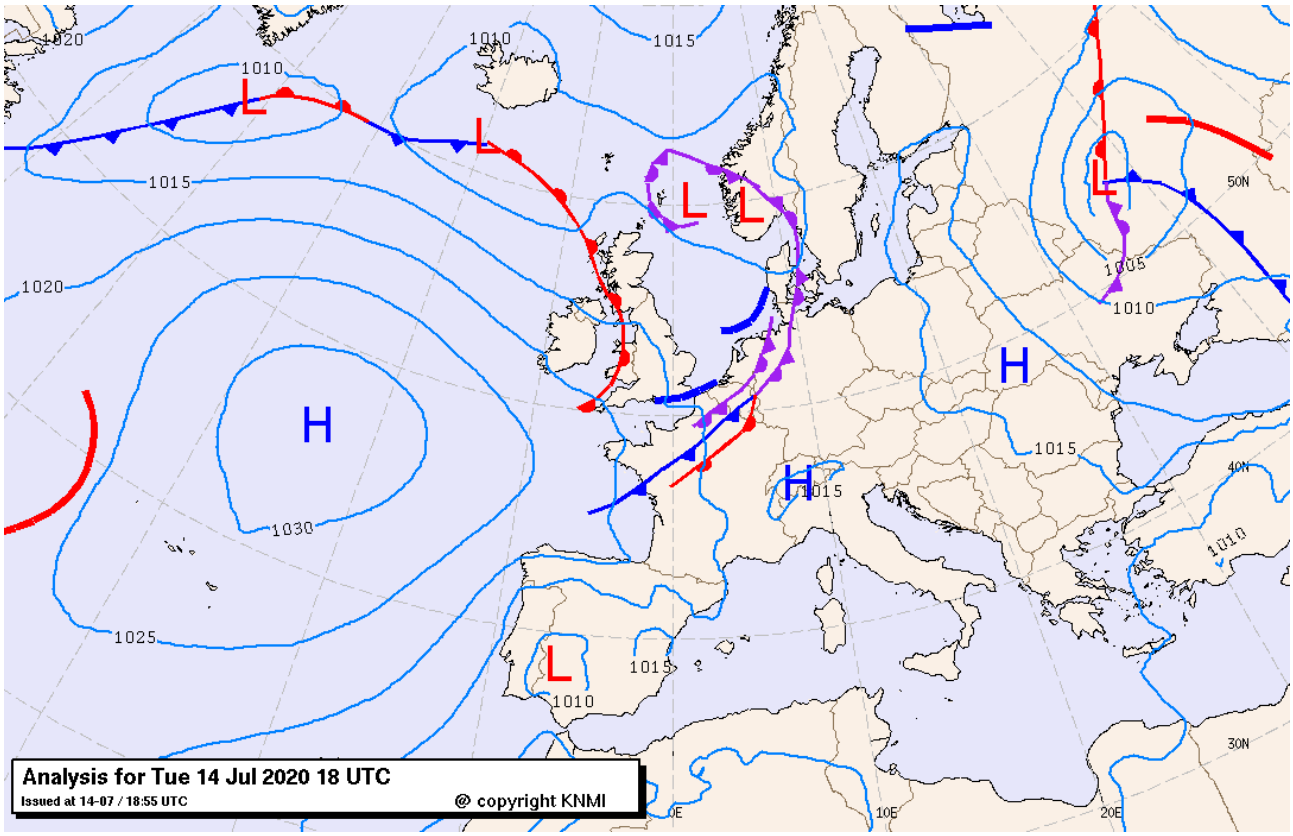

Figure 4. Surface pressure chart from KNMI data center. 14 July 2020 at 18 UTC.

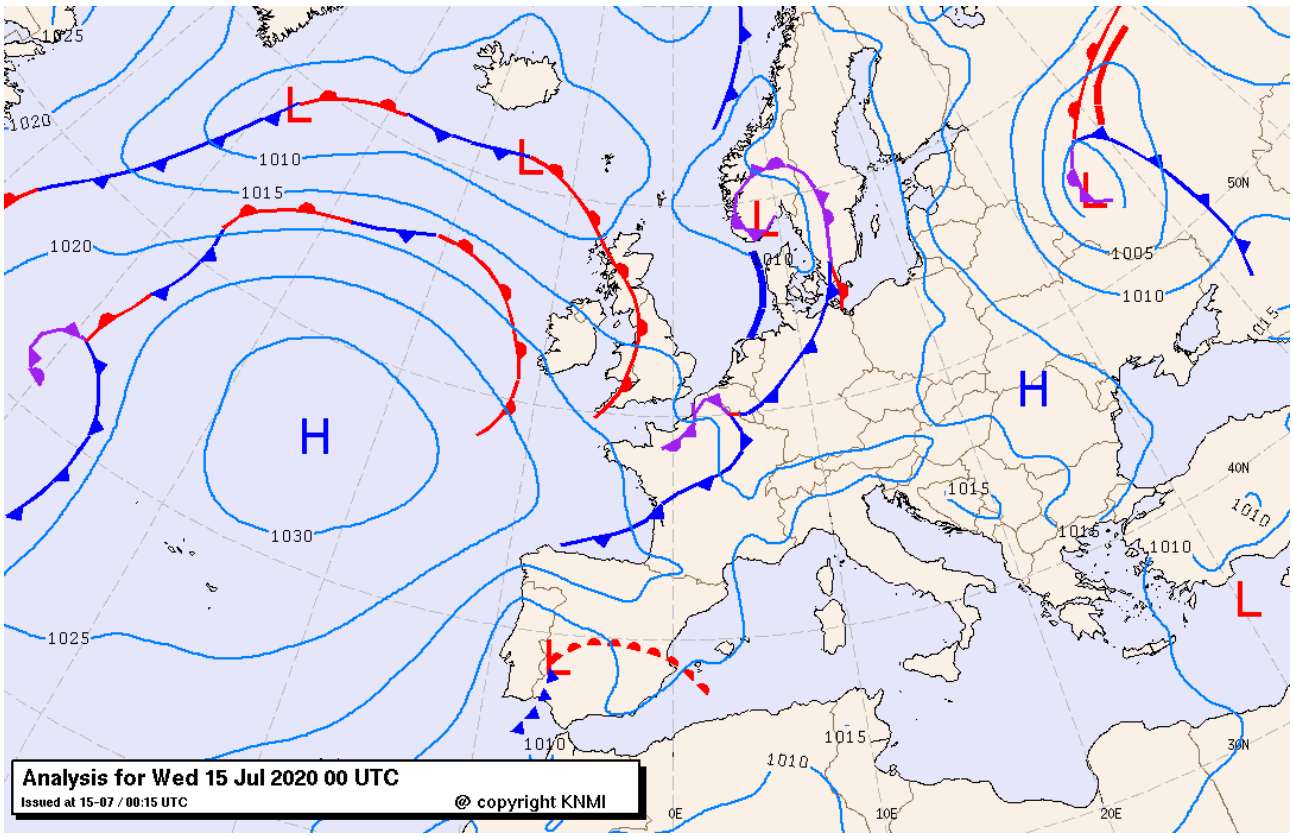

Figure 5. Surface pressure chart from KNMI data center. 15 July 2020 at 00 UTC.

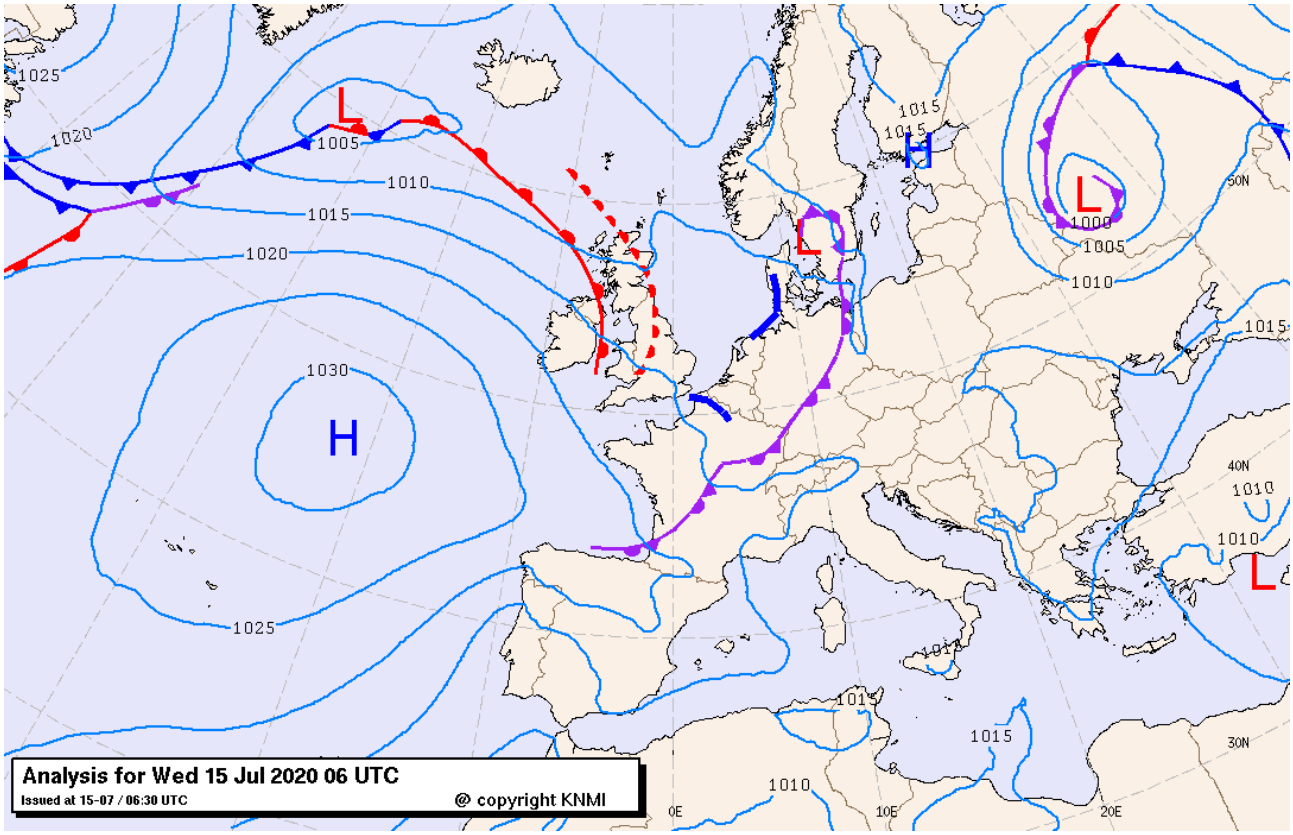

Figure 6. Surface pressure chart from KNMI data center. 15 July 2020 at 06 UTC.

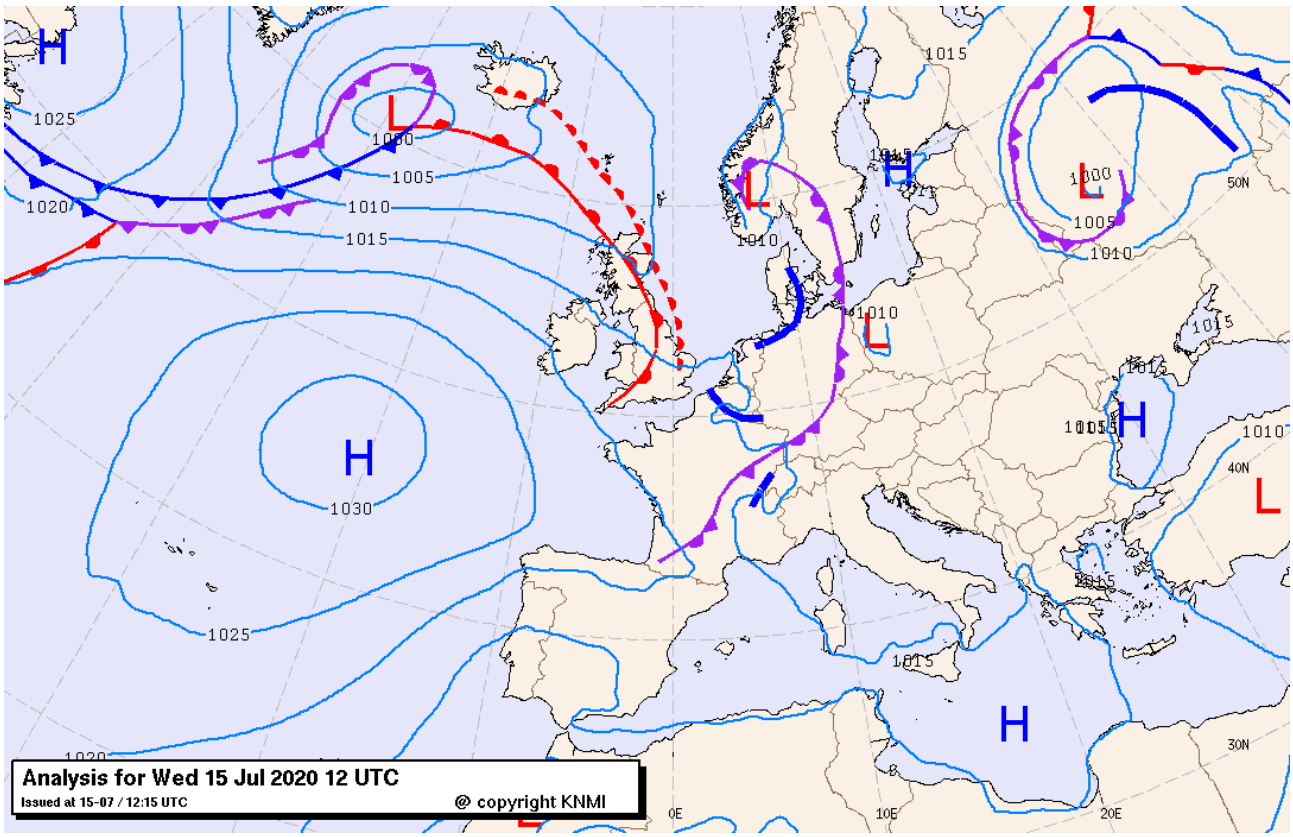

Figure 7. Surface pressure chart from KNMI data center. 15 July 2020 at 12 UTC.

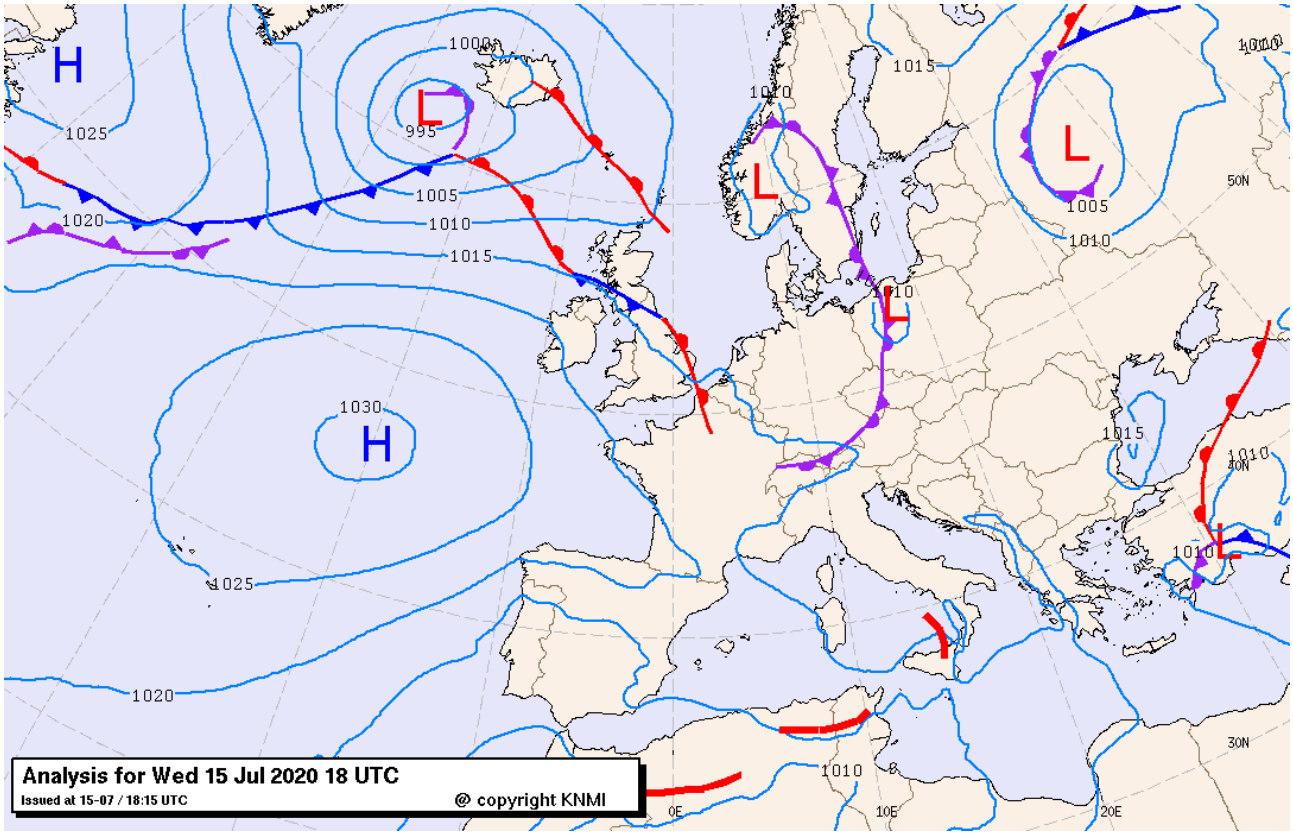

Figure 8. Surface pressure chart from KNMI data center. 15 July 2020 at 18 UTC.

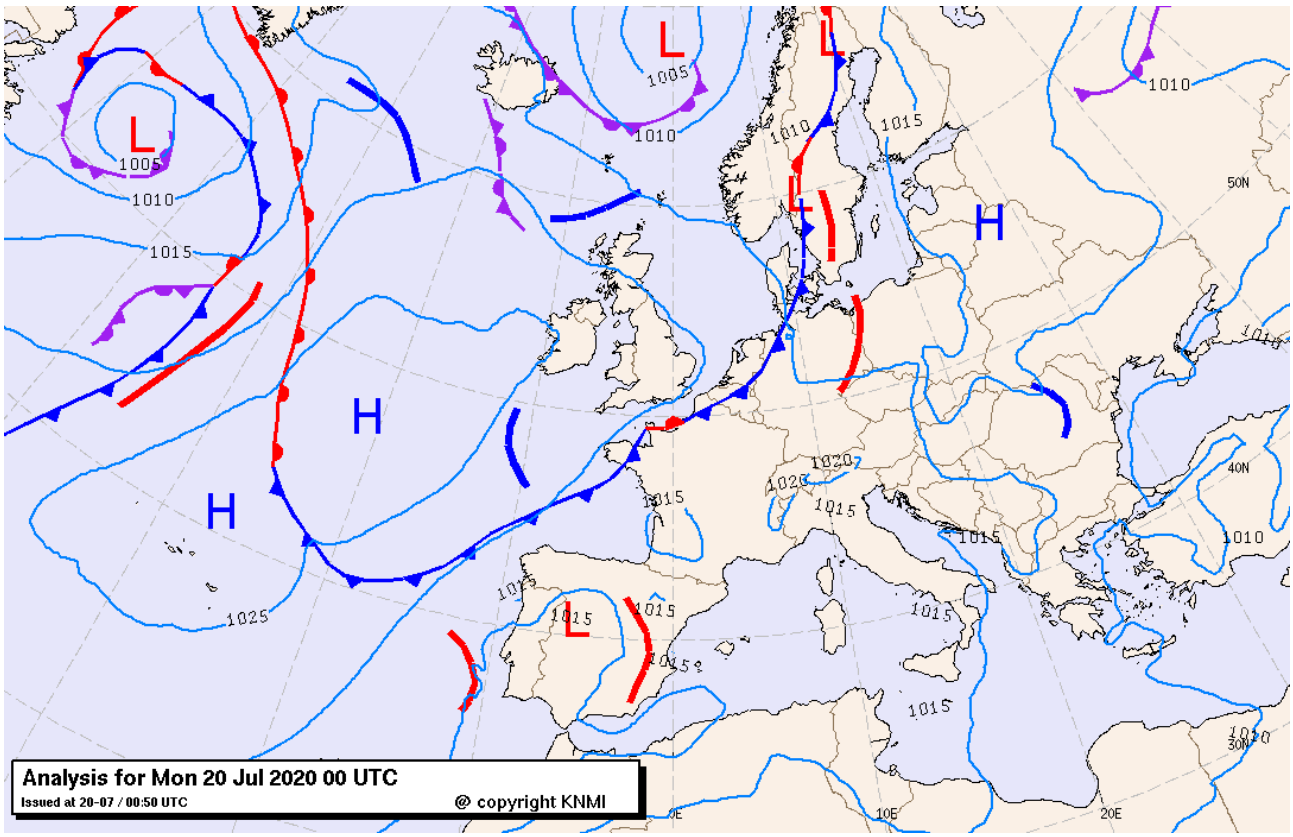

Figure 9. Surface pressure chart from KNMI data center. 20 July 2020 at 00 UTC.

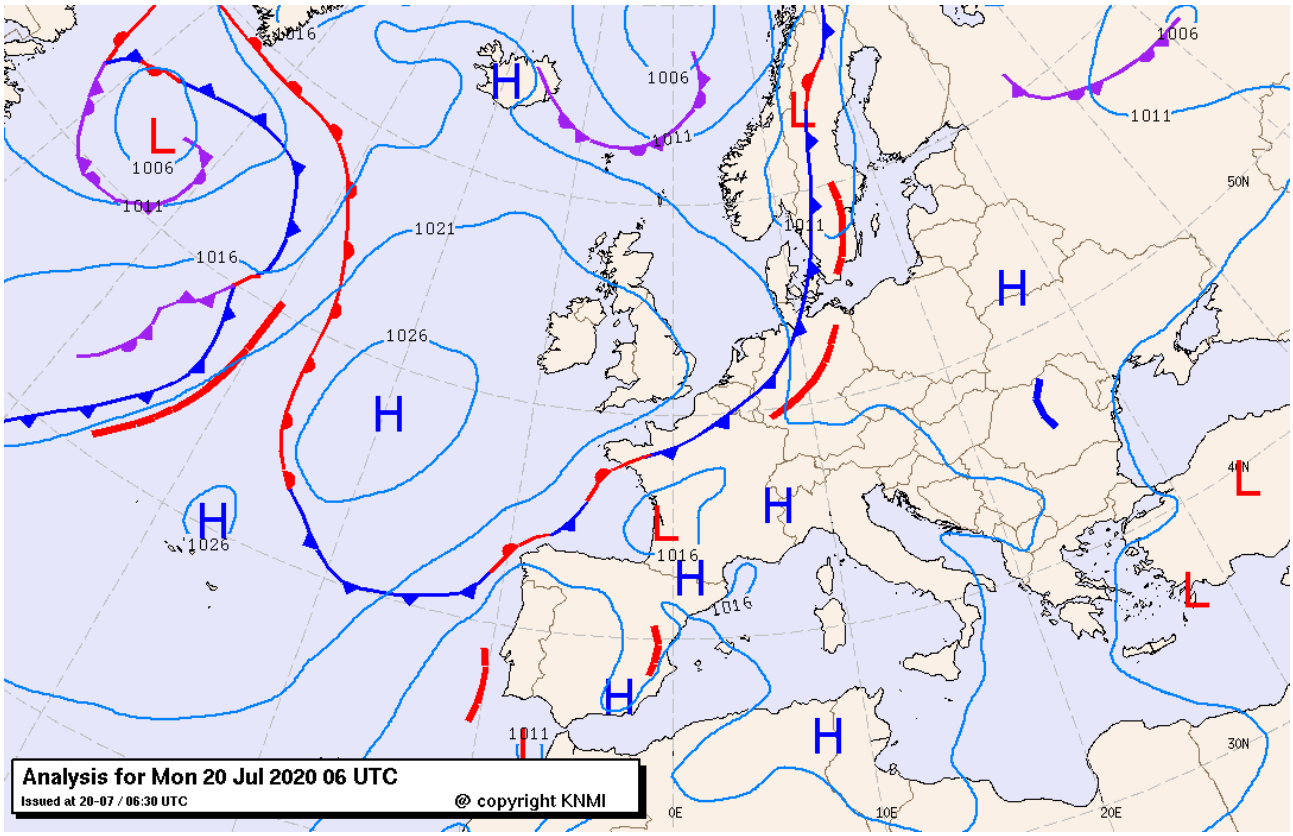

Figure 10. Surface pressure chart from KNMI data center. 20 July 2020 at 06 UTC.

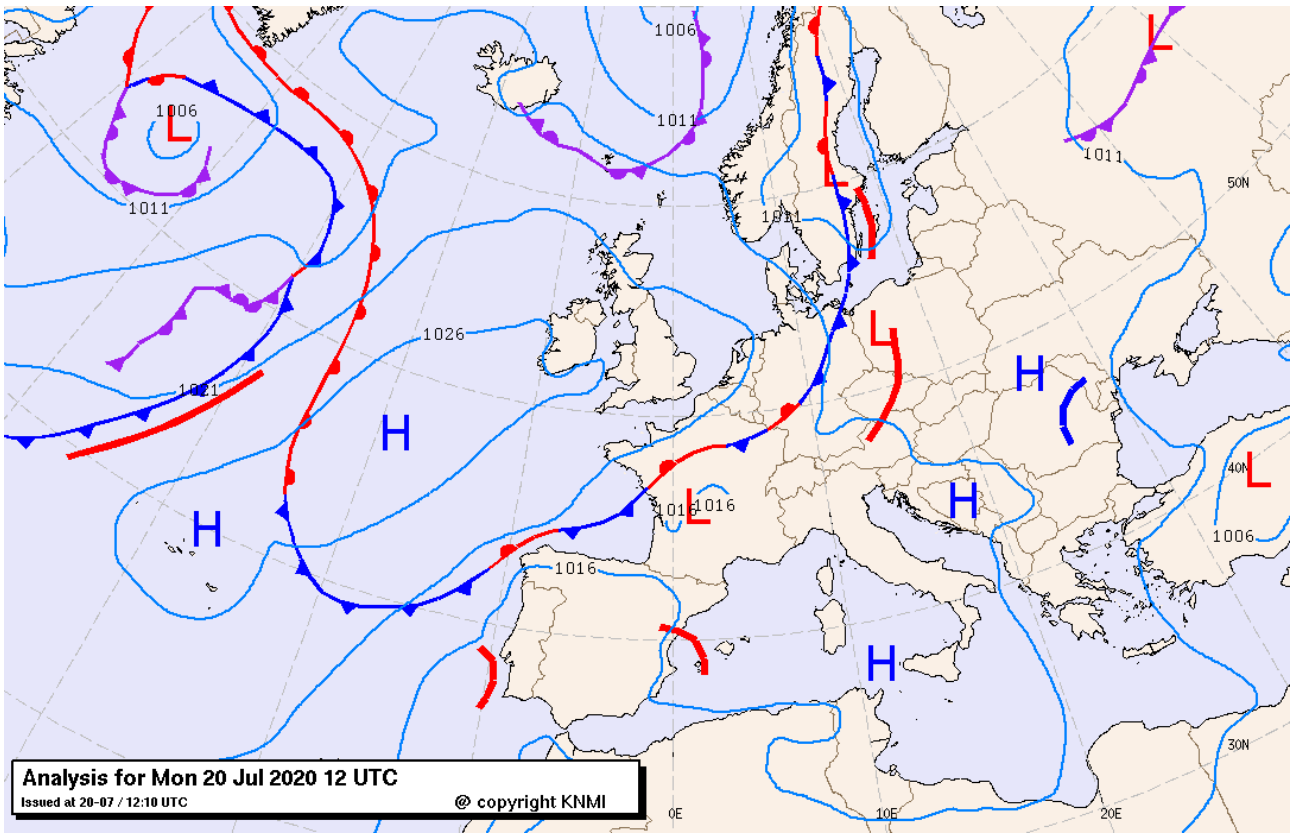

Figure 11. Surface pressure chart from KNMI data center. 20 July 2020 at 12 UTC.

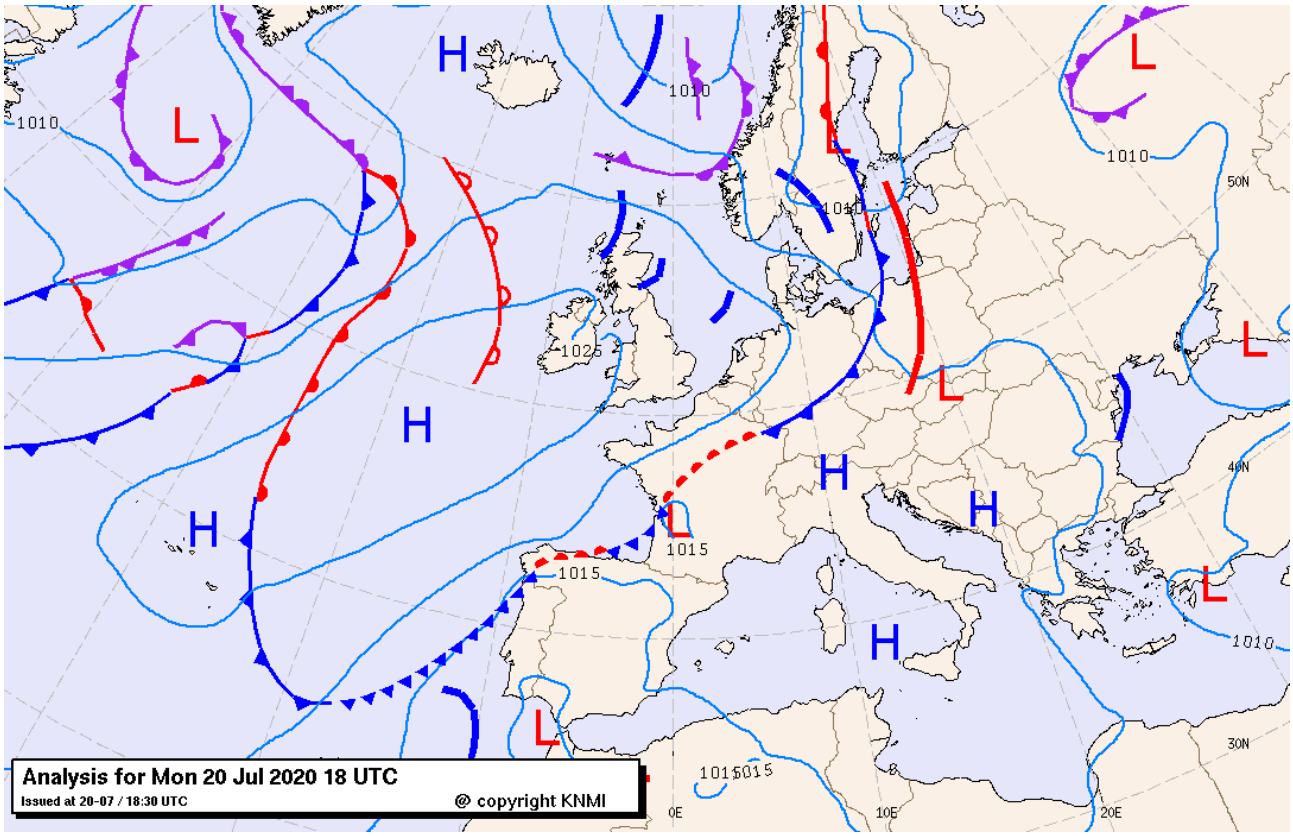

Figure 12. Surface pressure chart from KNMI data center. 20 July 2020 at 18 UTC.

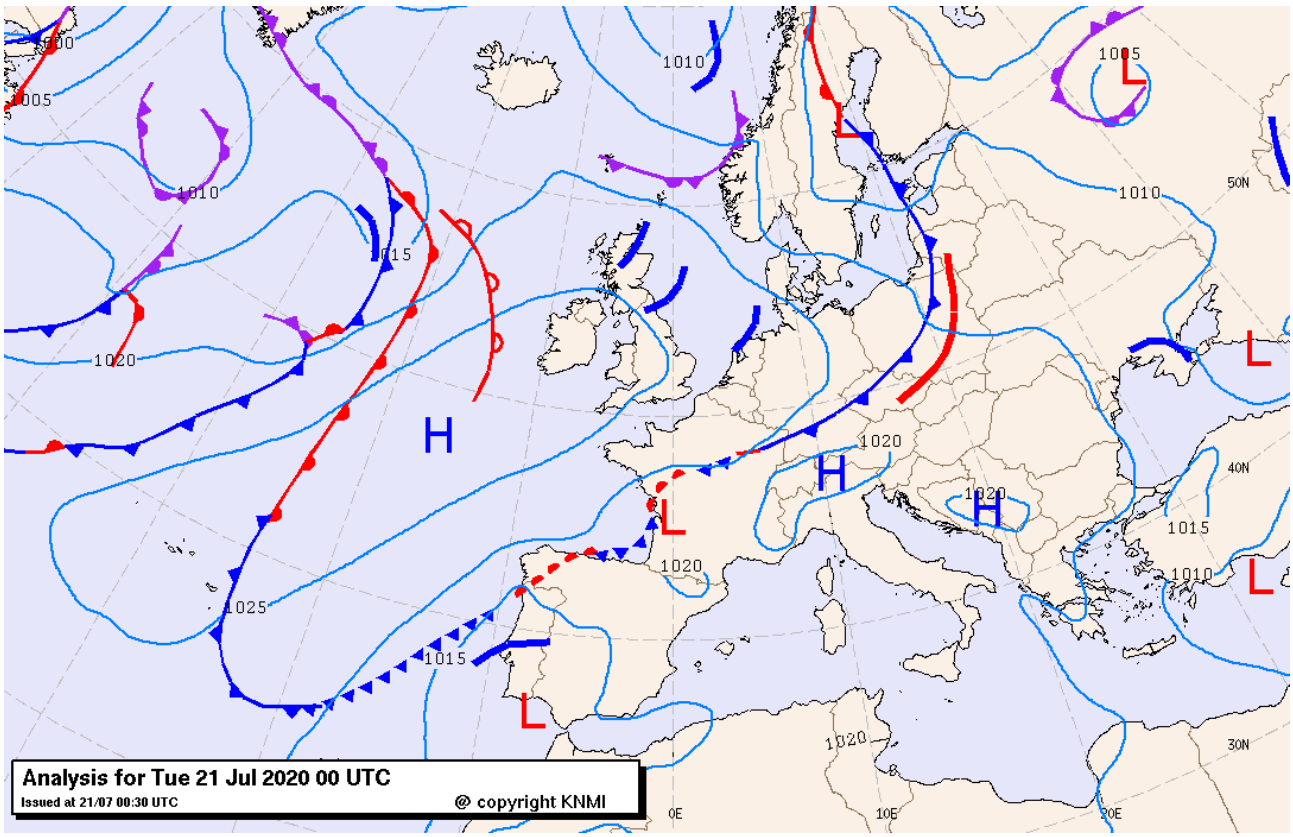

Figure 13. Surface pressure chart from KNMI data center. 21 July 2020 at 00 UTC.

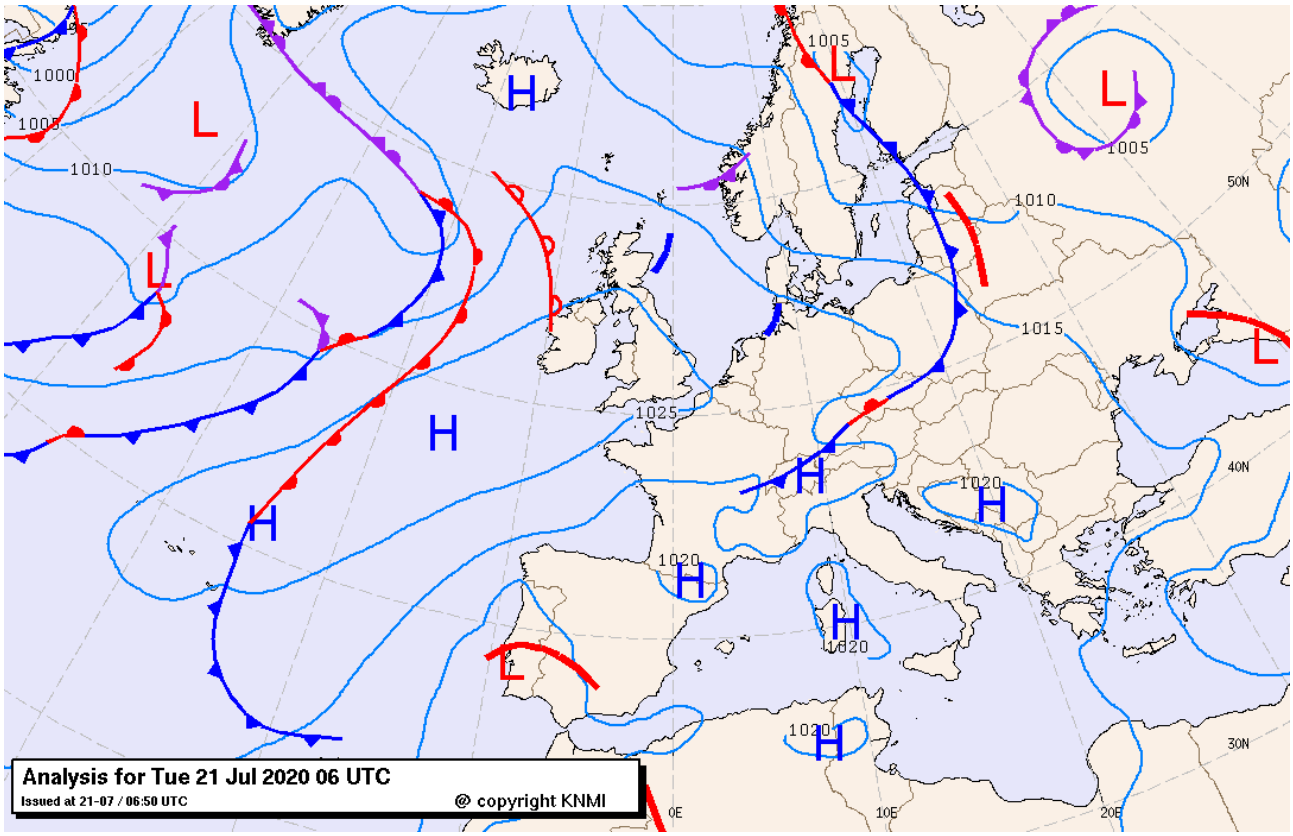

Figure 14. Surface pressure chart from KNMI data center. 21 July 2020 at 06 UTC.

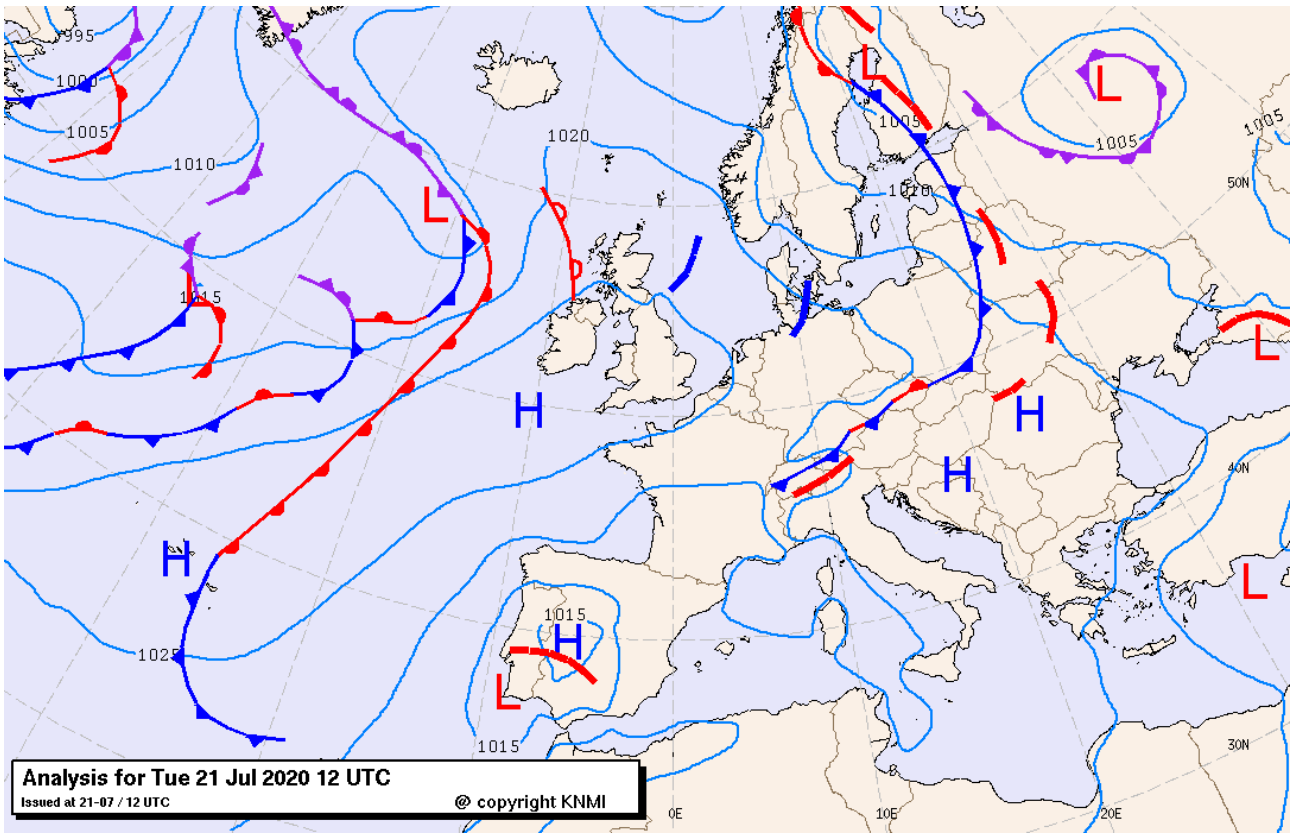

Figure 15. Surface pressure chart from KNMI data center. 21 July 2020 at 12 UTC.

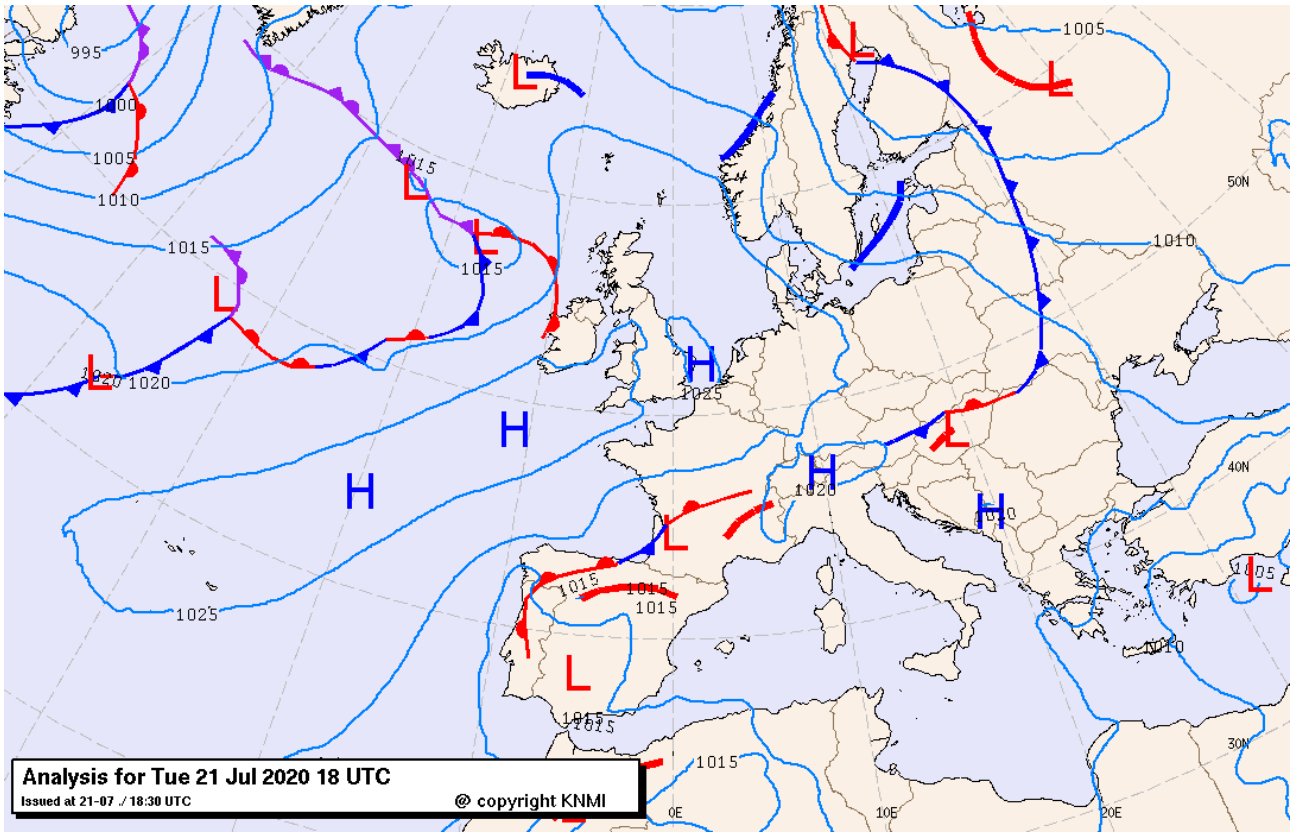

Figure 16. Surface pressure chart from KNMI data center. 21 July 2020 at 18 UTC.

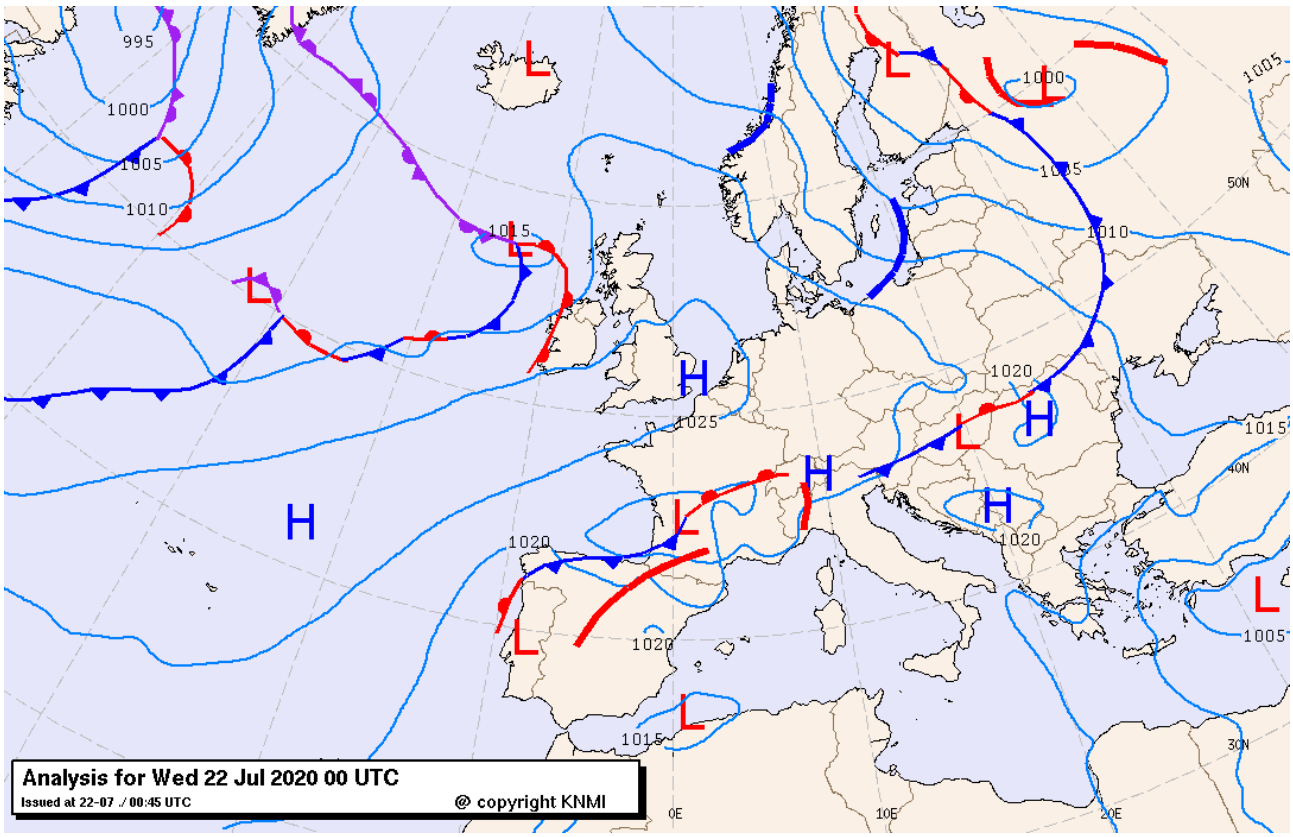

Figure 17. Surface pressure chart from KNMI data center. 22 July 2020 at 06 UTC.

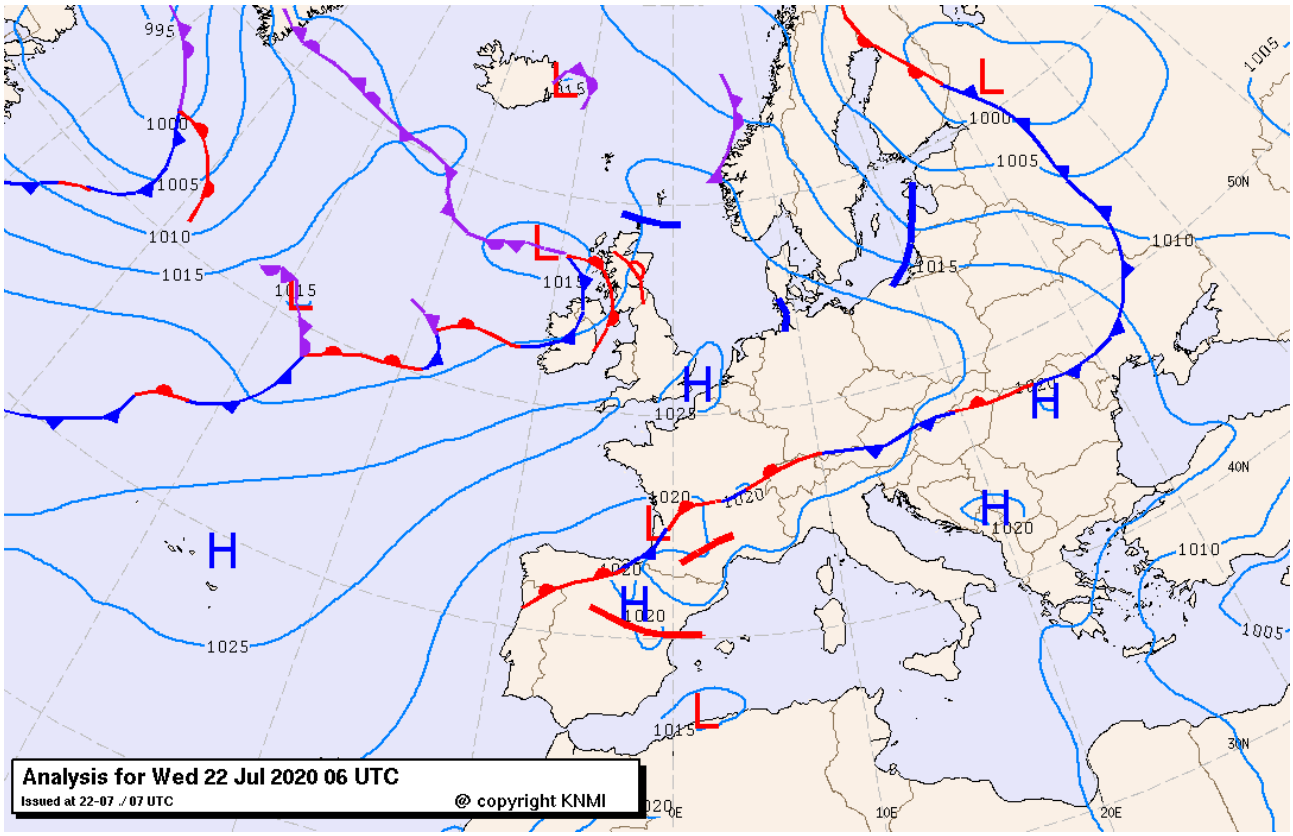

Figure 18. Surface pressure chart from KNMI data center. 22 July 2020 at 06 UTC.

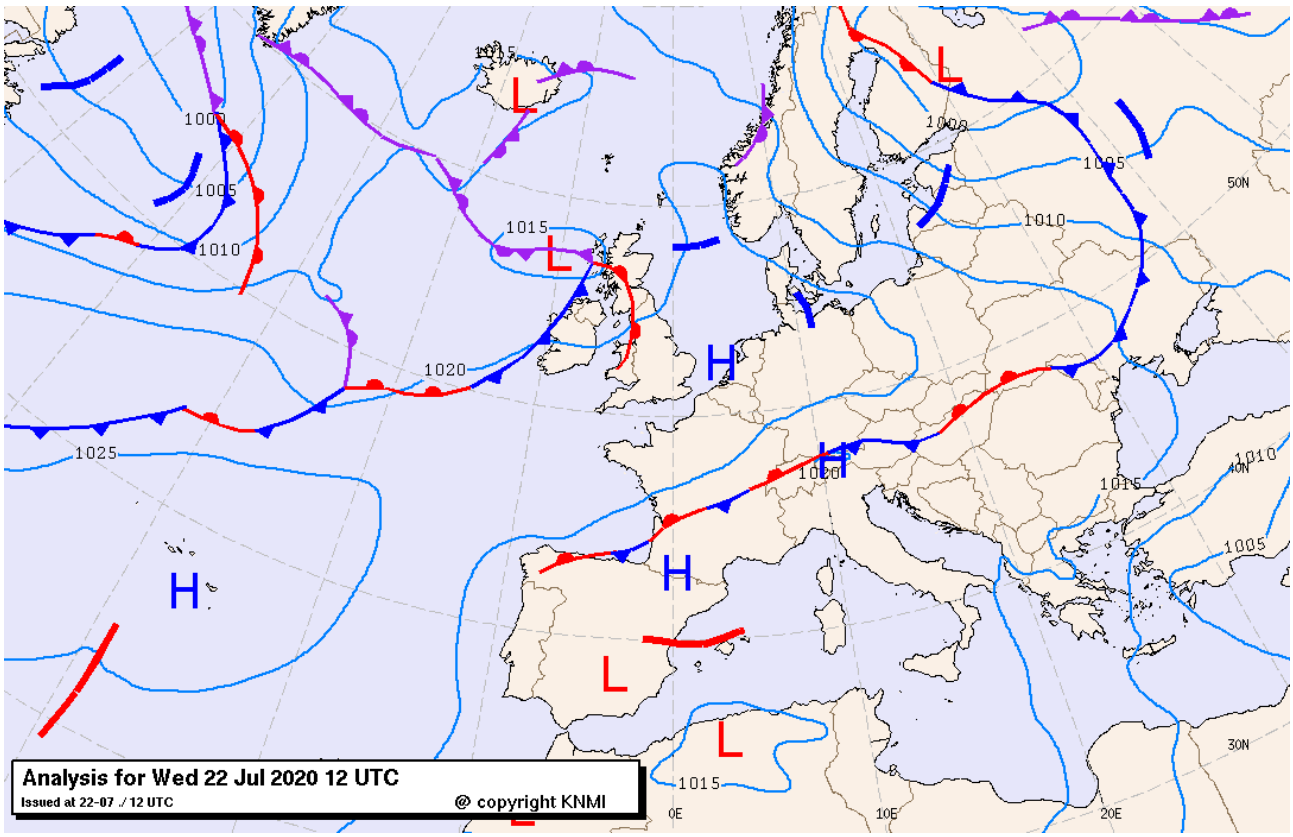

Figure 19. Surface pressure chart from KNMI data center. 22 July 2020 at 12 UTC.

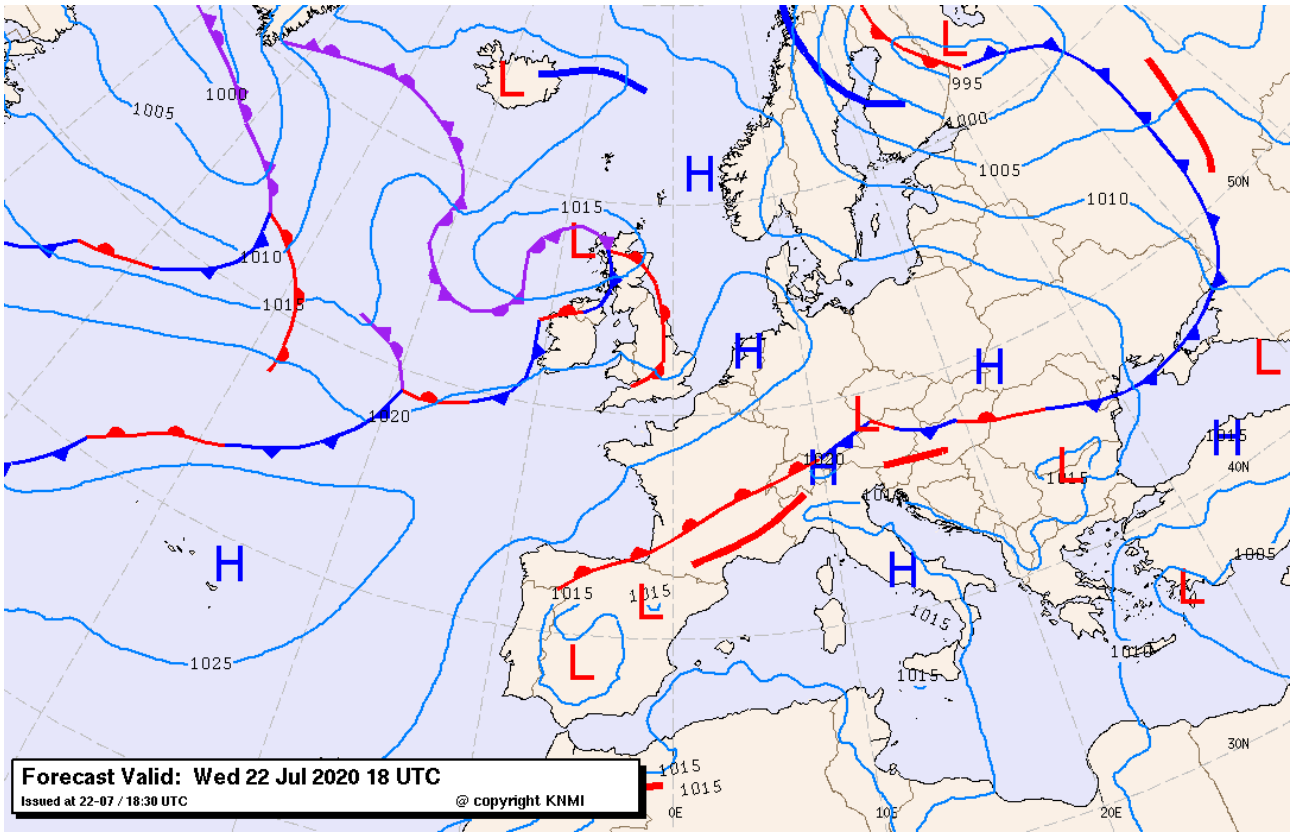

Figure 20. Surface pressure chart from KNMI data center. 22 July 2020 at 18 UTC.

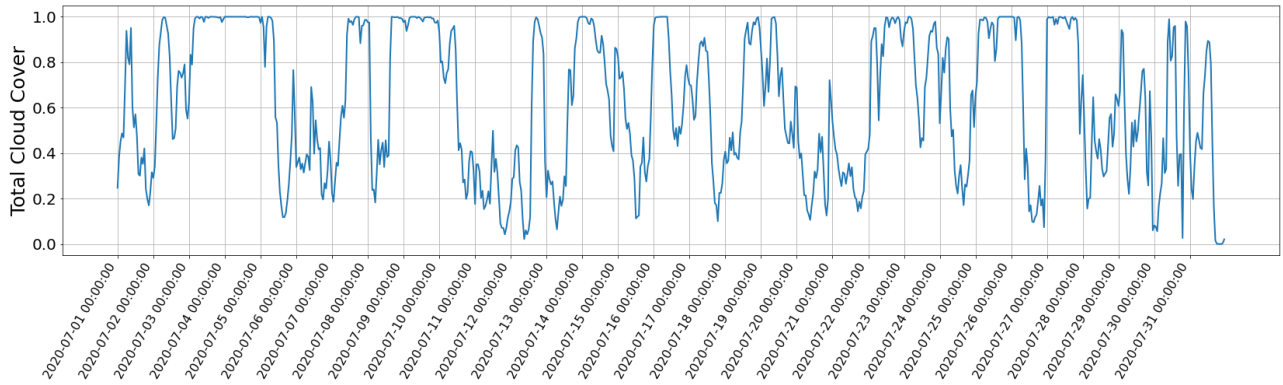

Figure 21. Time series of total cloud cover for Schiermonnikoog, 01 to 31 July 2020.

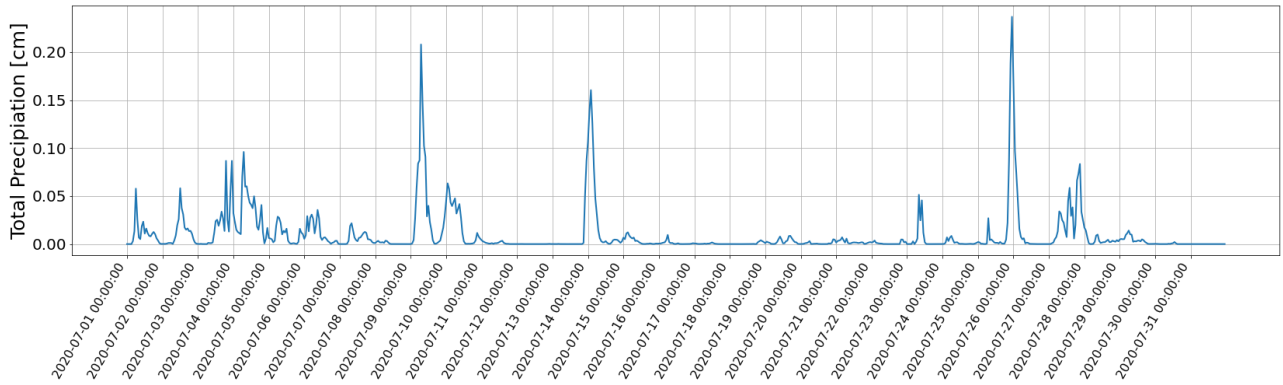

Figure 22. Time series of total precipitation for Schiermonnikoog, 01 to 31 July 2020.

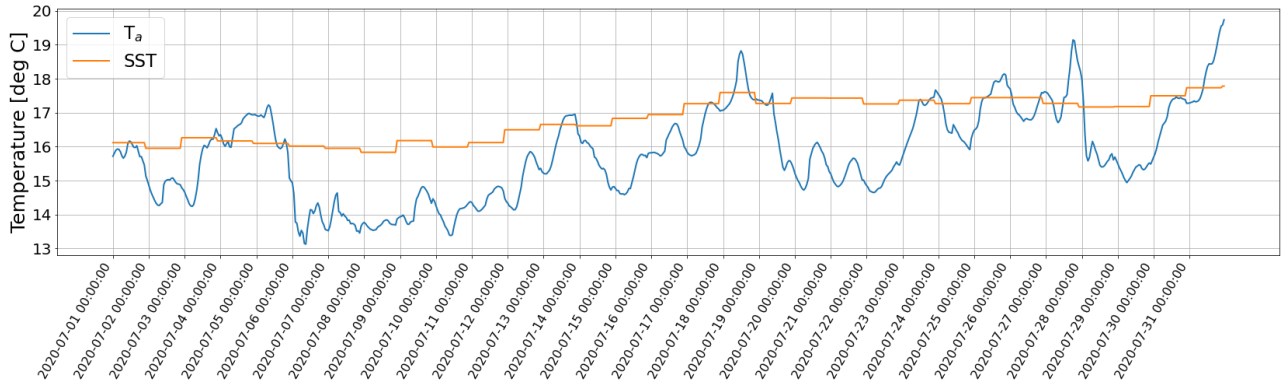

Figure 23. Time series of sea surface temperature and air temperature at 2 m for Schiermonnikoog, 01 to 31 July 2020.

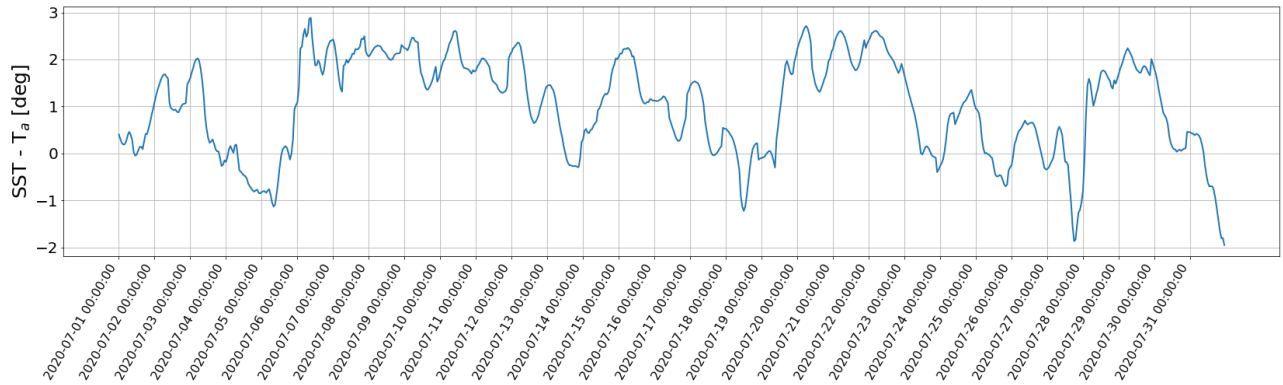

Figure 24. Time series of temperature difference for Schiermonnikoog, 01 to 31 July 2020.

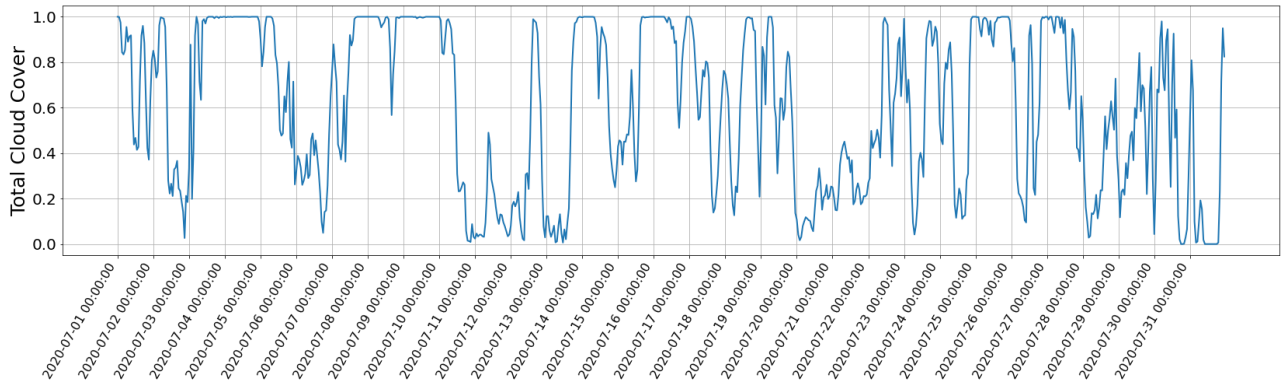

Figure 25. Time series of total cloud cover for IJmuiden, 01 to 31 July 2020.

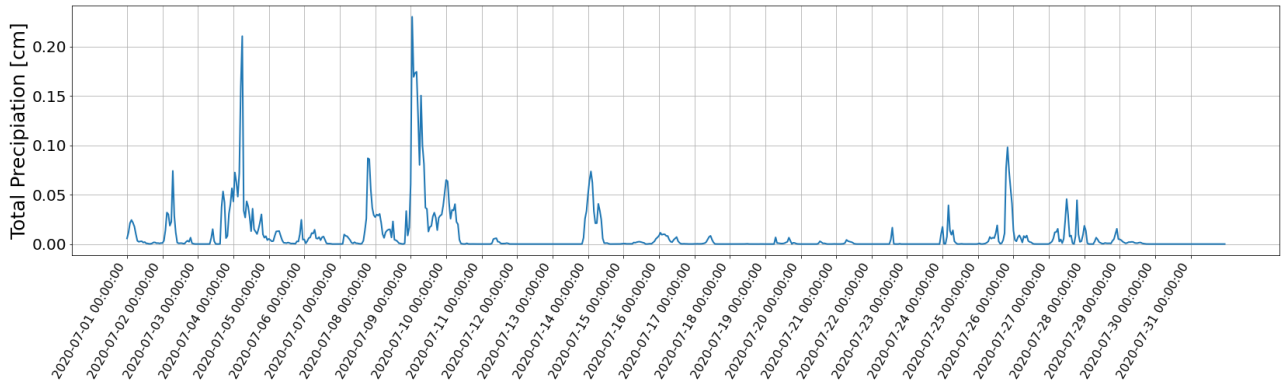

Figure 26. Time series of total precipitation for IJmuiden, 01 to 31 July 2020.

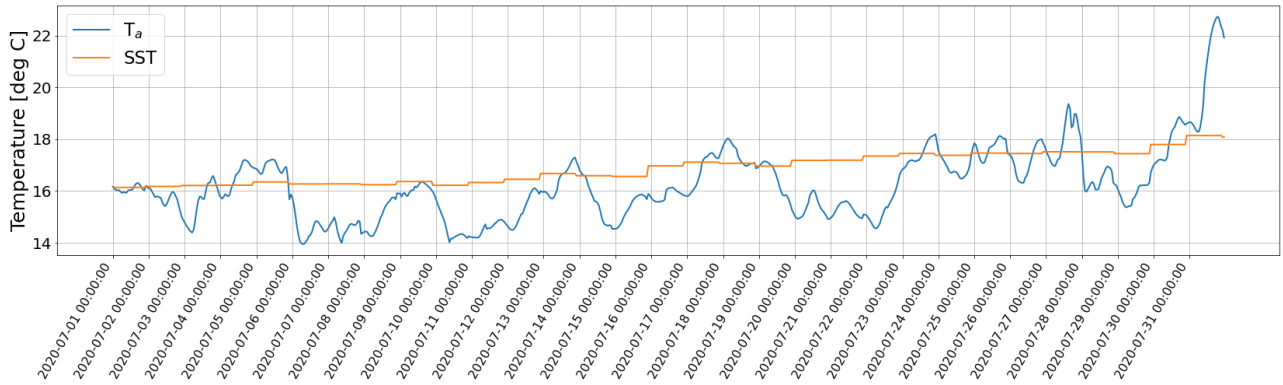

Figure 27. Time series of sea surface temperature and air temperature at 2 m for IJmuiden, 01 to 31 July 2020.

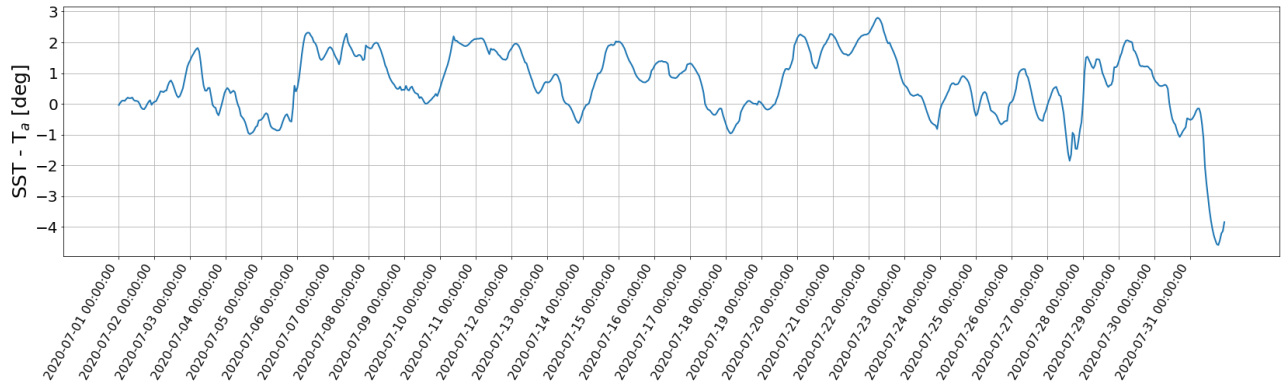

Figure 28. Time series of temperature difference for IJmuiden, 01 to 31 July 2020.

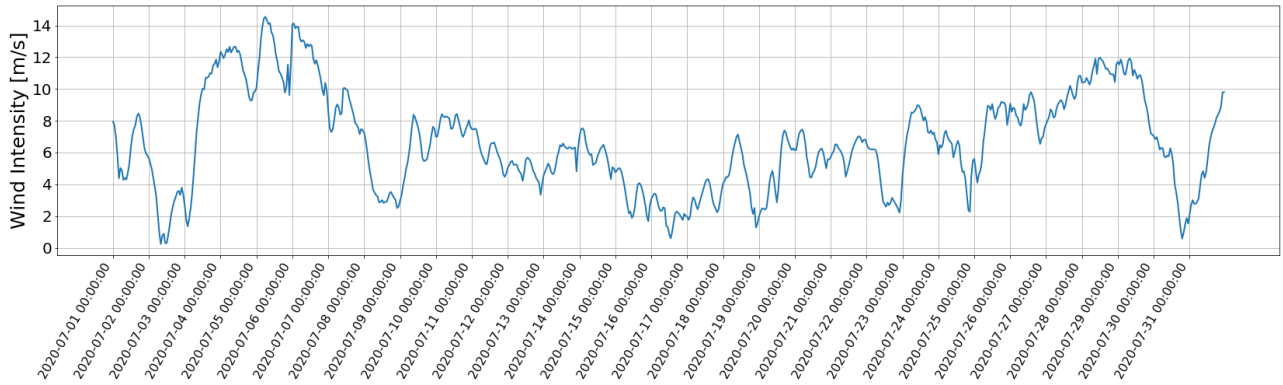

Figure 29. Time series of wind intensity at 10 m for Schiermonnikoog, 01 to 31 July 2020.

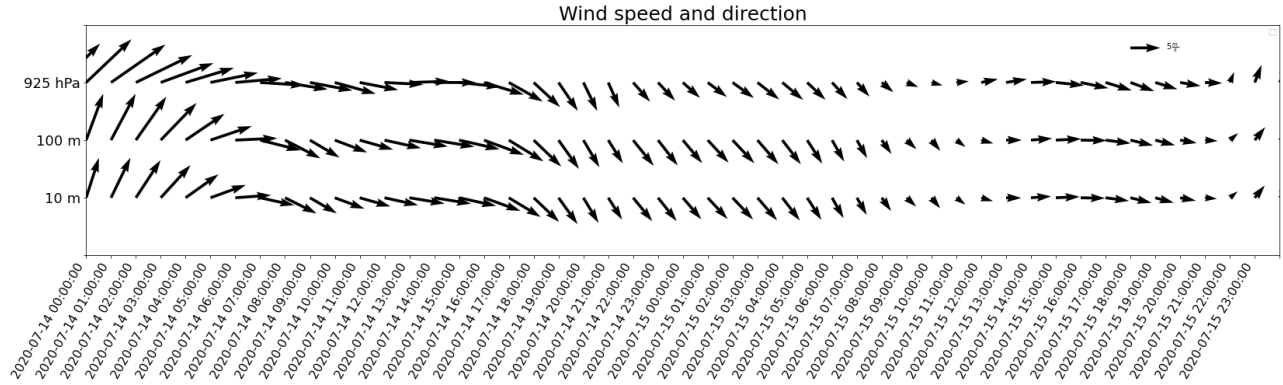

Figure 30. Time series of wind speed and direction at 10 m, 100 m, and at 925 hPa for Schiermonnikoog, 14-15 July 2020.

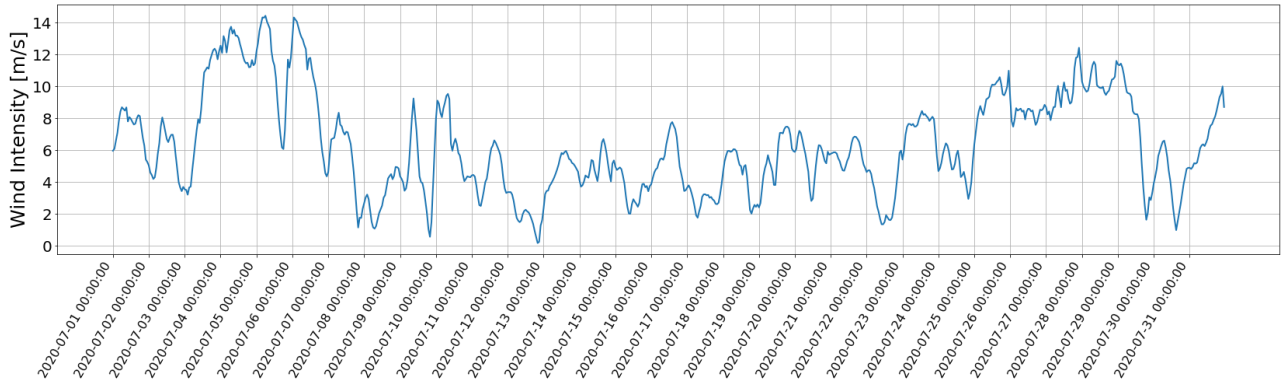

Figure 31. Time series of wind intensity at 10 m for IJmuiden, 01 to 31 July 2020.

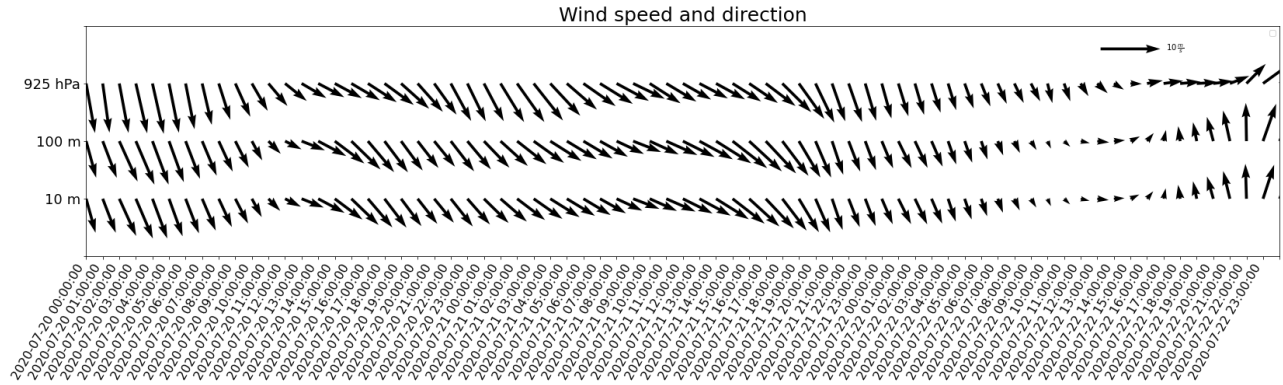

Figure 32. Time series of wind speed and direction at 10 m, 100 m, and at 925 hPa for IJmuiden, 20 to 22 July 2020.